We are IntechOpen,
the world's leading publisher of
Open Access books
Built by scientists, for scientists

6,900
Open access books available

186,000
International authors and editors

200M
Downloads

154
Countries delivered to

Our authors are among the
TOP 1%
most cited scientists

12.2%
Contributors from top 500 universities

CLARIVATE ANALYTICS
BOOK CITATION INDEX
INDEXED

WEB OF SCIENCE™
Selection of our books indexed in the Book Citation Index
in Web of Science™ Core Collection (BKCI)

Interested in publishing with us?
Contact book.department@intechopen.com

Numbers displayed above are based on latest data collected.
For more information visit www.intechopen.com

8

Automated MOS Transistor gamma Degradation Measurements Based on LabVIEW Environment

Slimane Oussalah and Boualem Djezzar
Centre de Développement des Technologies Avancées (CDTA)
Algeria

1. Introduction

In recent years, the study of the effects of ionizing radiation in thin gate oxides has received increasing attention. This is due not only to the appearance of new lithography tools for ultra low scale integration (ULSI) technologies, that use X- rays or e-beams, but also for the interest of space, medical, military or high-energy applications, where the complementary metal-oxide-semiconductor (CMOS) read-out circuitry will be subjected to a very hostile radiation environment.

A major concern in the reliability of metal-oxide-semiconductor field effect transistor (MOSFET) devices is the formation of interface traps and near-interface oxide traps; called also border traps; under hot carrier injection, irradiation and processing. Traps at or near the semiconductor/gate dielectric interface can cause degraded transconductance (Doyle et al., 1990), the shifting of threshold voltage (Tsuchiya et al., 1987) and may lead to dielectric breakdown (Chen et al., 1985). In order to improve the resistance of MOSFET devices to these effects, it is necessary to have a reliable method of determining the densities of both interface traps and oxide traps (Djezzar et al., 2004).

The reliable test procedure to predict radiation response of integrated circuits (IC's) from standard test laboratory, for example in space, is very important and requires a development of simple and rapid electrical characterization techniques easily mountable in production line. Therefore, intensive works have been carried out on the electrical characterization techniques for MOS gate oxide and Si/SiO_2 interface degradation caused by radiation (Schwank et al., 1993). The charge pumping (CP) technique (Groeseneken et al., 1984) is a valuable tool for all kind of traps characterization.

In this article, we present an automatic measurement bench programmable by the IEEE-488 bus that permits to characterize MOSFET device degradation induced by gamma radiation at low doses. This characterization permits to extract threshold voltage and flatband voltage for virgin and irradiated samples. Moreover, the determination of the breakpoint frequency that represents the limit between interface and border trap contributions to the charge trap is automatically extracted. The measurement bench is managed by a program, written by a graphical language LabVIEW. LabVIEW is a powerful, platform-independent, graphical programming development system which is ideally suited for data acquisition, storage, analysis, and presentation.

2. The LabVIEW environment

LabVIEW (short for Laboratory Virtual Instrumentation Engineering Workbench) is a program development application from National Instruments, much like various C or BASIC software development tools. It is, however, different from those applications in one important respect. LabVIEW uses a graphical language (G), to create programs in block diagram form while other programming tools use text-based languages. LabVIEW includes libraries of functions and development tools designed specifically for instrument control. It has application specific libraries for data acquisition, serial instrument control, data analysis, data presentation and data storage.

Nowadays, not only is LabVIEW everywhere (Fig. 1), but it offers something for every scientist and engineer. All levels of users, ranging from experienced to non-programmers, will benefit from the interactive, configurable tools, enabling LabVIEW to be used as a one integrated tool for measurement and automation throughout the design process.

The LabVIEW system provides an intuitive, graphical interface for the automated control of laboratory equipment. For each specific type of measurement, a virtual instrument (VI) is created. A VI can be regarded as the software equivalent of a single piece of laboratory test equipment, even though the measurement it represents may involve any number of different laboratory units.

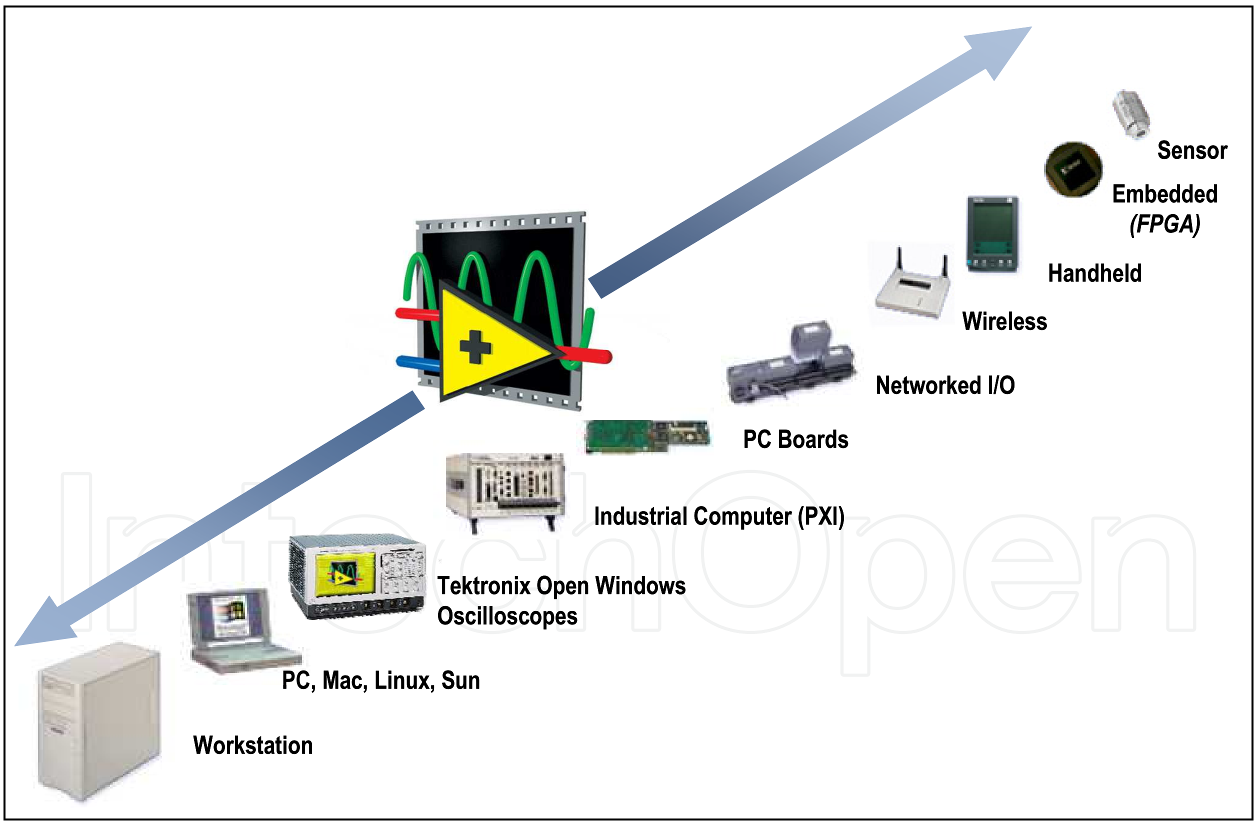

Fig. 1. LabVIEW is everywhere.

Each VI contains three main parts:
- Front Panel: how the user interacts with the VI.
- Block Diagram: the code that controls the program.
- Icon/Connector: Means of connecting a VI to other VIs.

All of the measurement parameters can be varied by manipulating a front panel (Fig. 2) which is the graphical equivalent of the push buttons and knobs on a test set, allowing a user who is not familiar with the programming to operate the setup easily

The Front Panel is used to interact with the user when the program is running. Users can control the program, change inputs, and see data updated in real time. Stress that controls are used for inputs- adjusting a slide control to set an alarm value, turning a switch on or off, or stopping a program. Indicators are used as outputs. Thermometers, lights, and other indicators indicate values from the program. These may include data, program states, and other information.

On the front panel of a VI, we place the controls and data displays for our system by selecting objects from the Controls palette, such as numeric displays, buttons, knobs, switches, meters, gauges, thermometers, tanks, LEDs, tables, arrays, charts, and graphs. When we complete and run the VI, we use the front panel to control our system whether we move a slide, zoom in on a graph, or enter a value with the keyboard. The front panel also serves to document the experiment; a hard copy yields results as well as all of the input parameters on one sheet.

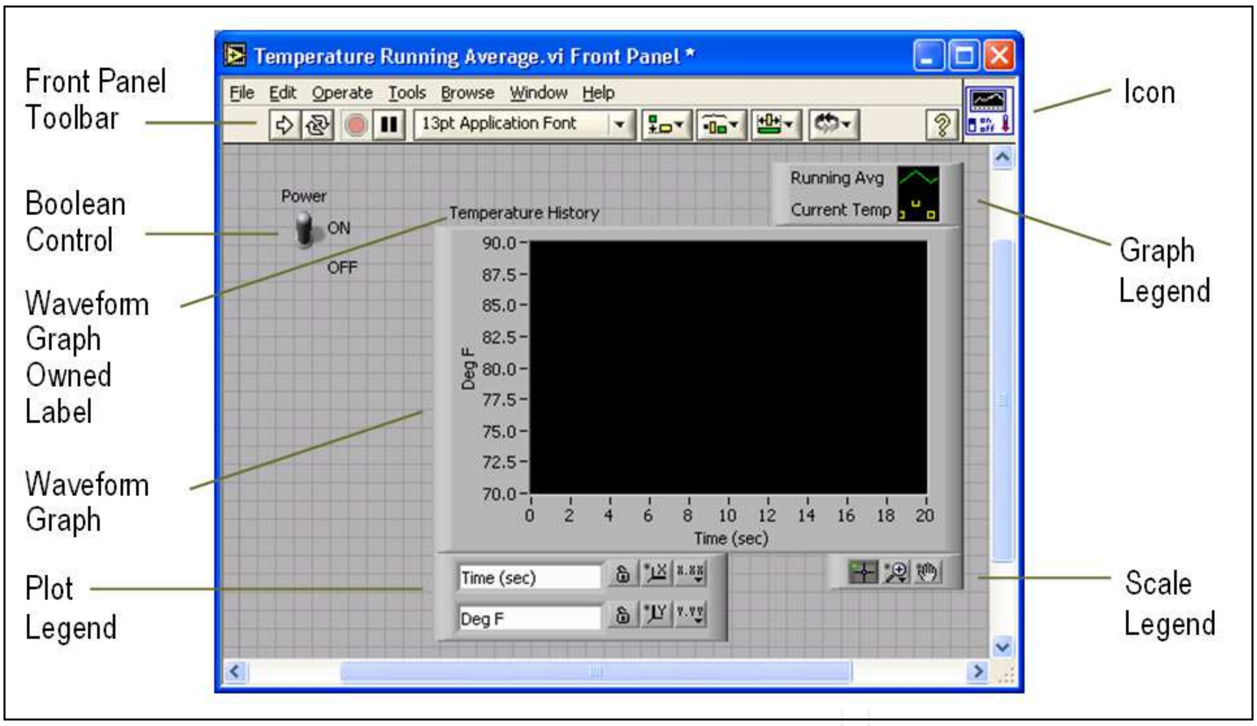
Front Panel Toolbar
Boolean Control
Waveform Graph Owned Label
Waveform Graph
Plot Legend
Icon
Graph Legend
Scale Legend
Temperature Running Average.vi Front Panel *
File Edit Operate Tools Browse Window Help
13pt Application Font
Power
ON
OFF
Temperature History
Running Avg
Current Temp
Deg F
90.0
87.5
85.0
82.5
80.0
77.5
75.0
72.5
70.0
0
2
4
6
8
10
12
14
16
18
20
Time (sec)
Time (sec)
Deg F

Fig. 2. LabVIEW front panel window.

The programming which coordinates the operation is accomplished graphically in the diagram panel Window using a dataflow language described by an example in Fig. 3.

To program the VI, we construct the block diagram without worrying about the syntactical details of text-based programming languages. We do this by selecting objects (icons) from the Functions palette and connecting them together with wires to transfer data among block diagram objects. These objects include simple arithmetic functions, Programming Structures, Signal Processing, advanced acquisition and analysis routines, network and file I/O operations, and more.

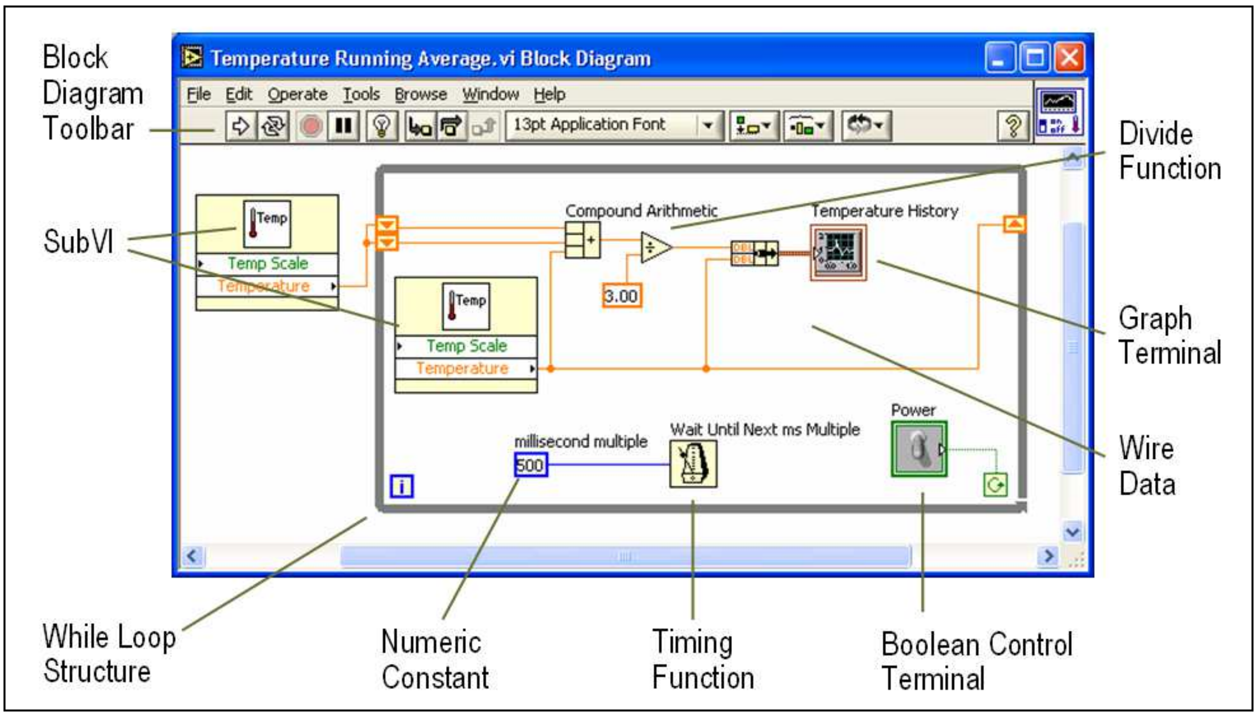
Block Diagram Toolbar
Temperature Running Average.vi Block Diagram
File Edit Operate Tools Browse Window Help
13pt Application Font
Divide Function
SubVI
Temp
Temp Scale
Temperature
Compound Arithmetic
Temperature History
3.00
Graph Terminal
Power
millisecond multiple
500
Wait Until Next ms Multiple
Wire Data
While Loop Structure
Numeric Constant
Timing Function
Boolean Control Terminal

Fig. 3. LabVIEW block diagram window.

3. Set-up and experimental procedure

3.1 Device and irradiation details

Samples investigated in this work are test structures, which were designed in Microelectronics and Nanotechnology Division of CDTA (Centre de Développement de Technologies Avancées) and fabricated in ES2 (European Silicon Structure) foundry. The different NMOS transistors within test structures were fabricated using a conventional (soft process) dual layer metal CMOS 2 µm N-well technology on p-type silicon <100> substrate with normal concentration of 7.6x1015 boron/cm^3, N+-poly-silicon gate, and 40 nm thick gate oxide layer grown in dry O$_2$. The gate capacitance per area unit, C$_{OX}$ is about of 8.6 10-8 F.cm^{-2}.
The radiation was performed at the CRS (Centre de Radioprotection et de Sureté) Laboratories, Algeria. Irradiation is performed at low doses up to 250 krad on non-packaged samples with gate lengths varying from 2µm to 20µm and width of 80 µm and 300 µm by using 1.25 MeV γ-rays at room temperature. The γ -ray was produced by 60Co cell with low-dose-rate of 200 rad/min. We have characterized the radiation effects at low doses on NMOS transistors. Thereafter, the electrical characterization is achieved by using standard charge pumping technique (CP) at high frequencies.

3.2 Experimental set-up

The experimental set-up details of the standard CP technique are shown in Fig. 4. The MOSFET source/drain terminals have been grounded, the gate terminal has been pulsed by applying a triangular pulse train with amplitude ΔV_G of various frequencies, and the substrate terminal has been grounded via a pico-ammeter. The measurements have been performed at room temperature and by using a sensitive Keithley 617 electrometer, Keithley 3940 multifunction synthesizer, and Karl Suss PA300 micro-manipulator semi-automatic probe station.

For all measurements, a reverse bias is applied to the source and the drain diodes. When the gate is pulsed between inversion and accumulation conditions (from above the threshold

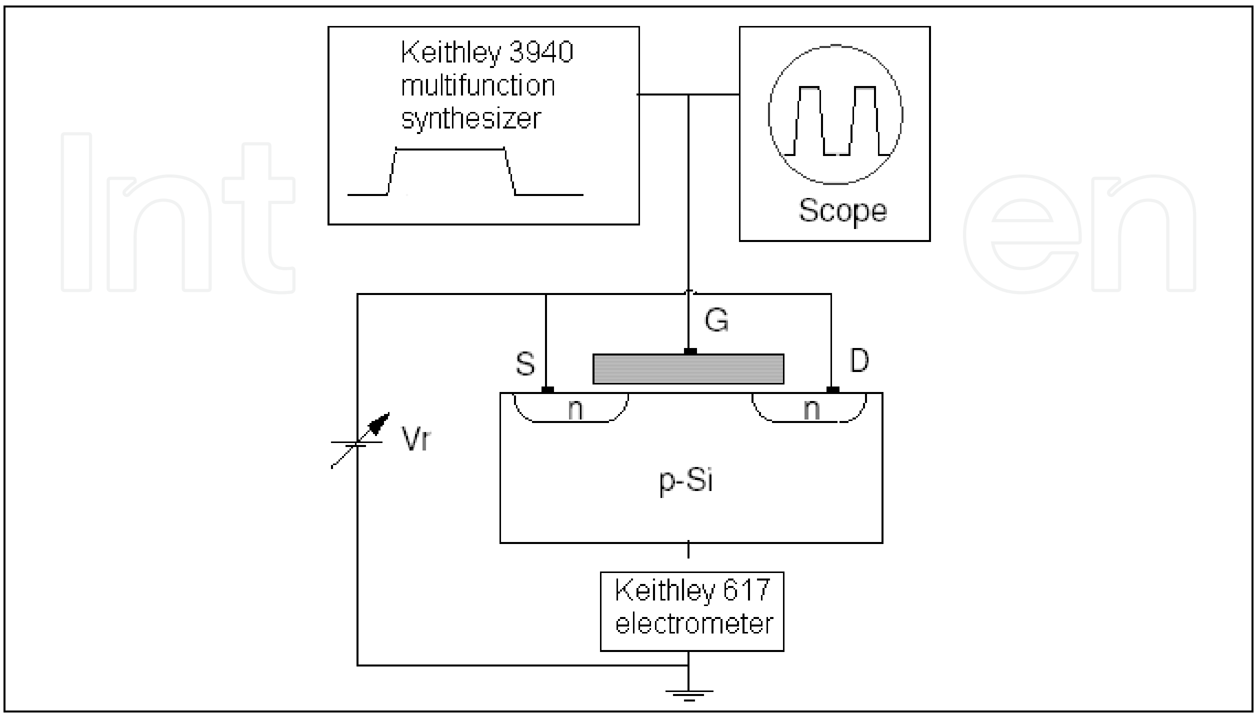
Keithley 3940
multifunction
synthesizer
Scope
G
S
D
n
n
Vr
p-Si
Keithley 617
electrometer

Fig. 4. Experimental setup for charge pumping measurement.

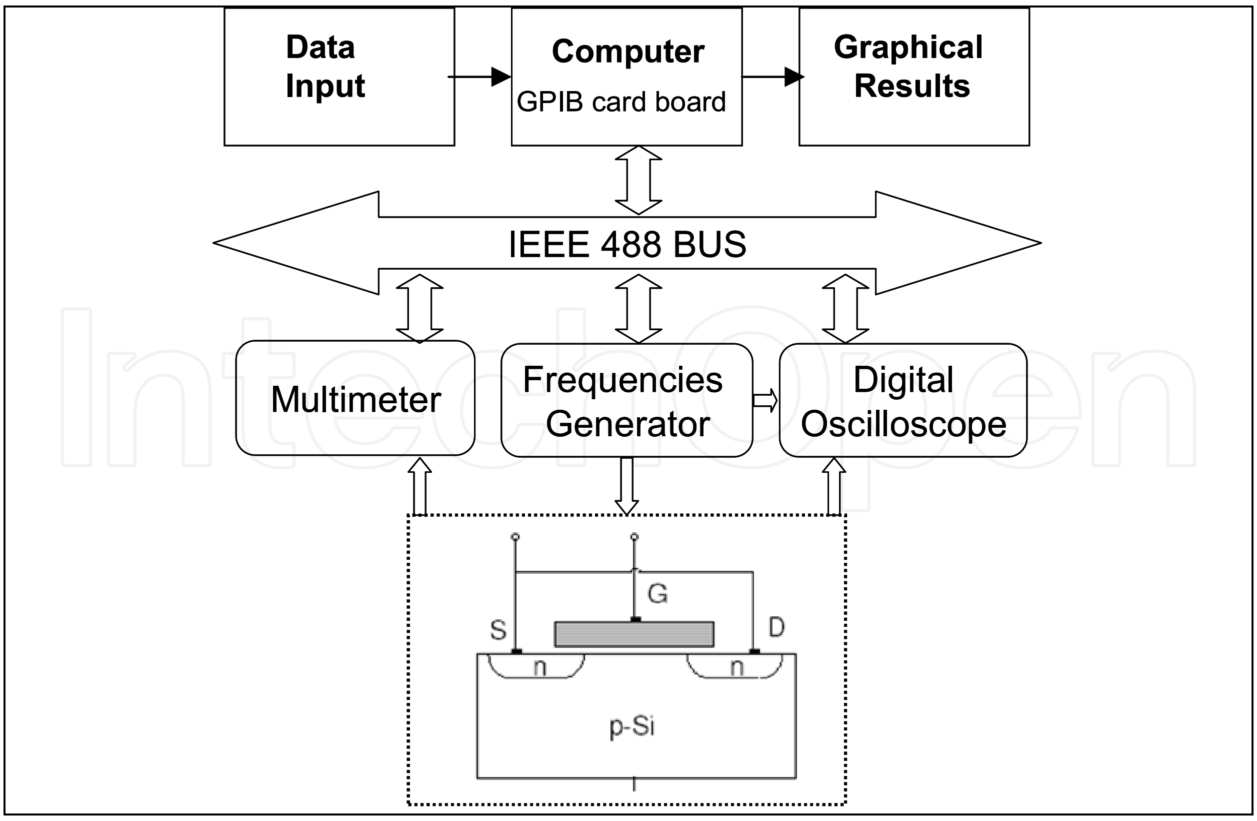
Data Input
Computer
GPIB card board
Graphical Results
IEEE 488 BUS
Multimeter
Frequencies Generator
Digital Oscilloscope
G
S
D
n
n
p-Si

Fig. 5. Description of the automatic measurements bench.

voltage to below the flatband voltage), trapping and recombination of carriers under these non equilibrium conditions gives rise to a net DC current that can be measured at the substrate. For relatively high frequency pulses (1 MHz), the CP current is proportional to the average density of interface traps which are physically located within 1 nm of the semiconductor –dielectric interface (Paulsen et al., 1992).

The test circuit chip within the probe station were isolated from vibration and enclosed in a grounded faraday box to avoid both RF and light effects. A computer has been programmed to control the measurement system, record the data, and extract the parameters. The control of instruments has been realized by a program developed with the LabVIEW software via the GPIB IEEE-488 bus.

Since the whole system is in this case based on computer (Fig. 5), the data is easily ported in ASCII form to other programs or even shared via networking with other machines.

4. Theoretical background

A commonly used definition of threshold voltage is that gate voltage for which the surface potential (ϕ_S) in the semiconductor below the gate oxide is given by:

$$\phi_S = 2\phi_F \tag{1}$$

where ϕ_F (V) is the Fermi level potential.

Thus, the threshold voltage (Schroder, 1998) is given as follows:

$$V_{th} = \phi_{MS} + 2\phi_F + \frac{\sqrt{2q\varepsilon_{si}N_A\left(2\phi_F\right)}}{C_{ox}} - \frac{Q_{total}}{C_{ox}} \tag{2}$$

where,

q (C) is the electron charge,

ε_{si} (F/cm) is the permittivity of silicon,

N_A (cm^{-3}) is the substrate doping,

C_{OX} (F/cm^2) is the gate oxide capacitance per area unit,

ϕ_{MS} (V) is the metal-semiconductor work function difference,

Q_T (C/cm^2) is the total charge density in SiO_2/Si system.

According to the Deal nomenclature (Deal, 1980), there are four general types of charges associated with the SiO_2/Si system. Fleetwood (Fleetwood, 1992) has completed this picture of charges by introducing a new charge type termed border trapped charge (Q_{BT}) as illustrated in Fig. 6. Thus Q_T is given by (Djezzar et al., 2004):

$$Q_T = Q_F + Q_M + Q_{OT} + Q_{IT} + Q_{BT} \tag{3}$$

where,

Q_F (C/cm^2) is the fixed charge density,

Q_M (C/cm^2) is the mobile oxide charge density,

Q_{OT} (C/cm^2) is the oxide-trapped charge density,

Q_{IT} (C/cm^2) is the interface-trapped charge density,

Unlike fixed oxide charge, oxide trapped charge, and mobile oxide charge, interface trapped charge is in electrical communication with the underlying silicon. by substituting eq. (3) in eq. (2), V_{TH} can be written as:

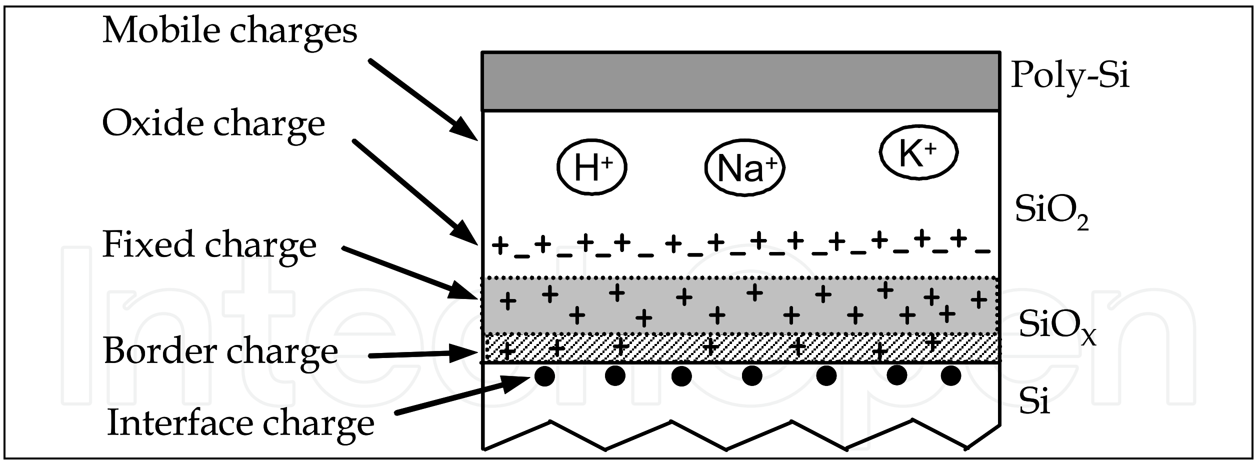

Fig. 6. Schematic illustration of different charges in MOS devices.

$$V_{TH} = \phi_{MS} + 2\phi_F + \frac{\sqrt{2q\varepsilon_{Si}N_A(2\phi_F)}}{C_{OX}} - \frac{1}{C_{OX}}(Q_F + Q_M + Q_{OT} + Q_{IT} + Q_{BT}) \tag{4}$$

When MOS transistors are exposed to various types of stress such as ionizing radiation, FN injection, or hot carrier injection, the gate oxide and SiO_2/Si interface are damaged. This degradation is induced by the creation of oxide-trapped charge (ΔQ_{OT}) and interface trapped charge (ΔQ_{IT}). The different charge increments are shown in fig. 2. Contrary to Q_{OT}, Q_{IT}, and and Q_{BT}, Q_F and Q_M are not affected by these ionizing stresses. Consequently, the threshold voltage shift caused by uniform stresses (FN stress or radiation effect) is given by:

$$\Delta V_{TH} = -\frac{\Delta Q_{IT}}{C_{OX}} - \frac{\Delta Q_{OT}}{C_{OX}} - \frac{\Delta Q_{BT}}{C_{OX}} \tag{5}$$

where,
ΔQ_{IT} ($C.cm^{-2}$) is the radiation-induced interface trapped charges,
ΔQ_{BT} ($C.cm^{-2}$) is the radiation-induced border trapped charges,
ΔQ_{OT} ($C.cm^{-2}$) is the radiation-induced oxide trapped charges.

Generally, the net radiation-induced oxide and border charges, ΔQ_{OT} and ΔQ_{BT} respectively, are positive and induce a negative shift in V_{TH}. However, ΔQ_{IT} can contribute either a net-negative or net-positive charge, depending on the position of the Fermi level at the silicon surface in inversion mode. Usually, the interface-trap is considered like an acceptor state for NMOS transistor and like a donor state for PMOS transistor. Therefore, ΔQ_{IT} is negative for n-channel ($\Delta Q_{IT} = -q\ \Delta N_{IT}$) and positive for p-channel ($\Delta Q_{IT} = q\ \Delta N_{IT}$) devices (Oldham, 1999). On the other hand, $\Delta Q_{OT} = q\ \Delta N_{OT}$ and $\Delta Q_{BT} = q\ \Delta N_{BT}$. Where ΔN_{IT}, ΔN_{OT}, and ΔN_{BT} are positive numbers per area unit.

So, ΔV_{TH} reads:

$$\Delta V_{TH} = \Delta V_{IT} + \Delta V_{OT} + \Delta V_{BT} \tag{8}$$

where,

$\Delta V_{IT} = -\Delta Q_{IT} / C_{OX} = q\ \Delta N_{IT} / C_{OX}$ (V) is the voltage shift caused by interface- trap increase,
$\Delta V_{OT} = -\Delta Q_{OT} / C_{OX} = -q\ N_{OT} / C_{OX}$ (V) is the voltage shift caused by oxide-trap increase,
$\Delta V_{BT} = -\Delta Q_{BT} / C_{OX} = -q\ \Delta N_{BT} / C_{OX}$ (V) is the voltage shift caused by border- trap increase.
The Equation 6 is only true when applying a DC signal or a low frequencies (less than a few kHz) AC signal train. Therefore, only ΔN_{OT} and ΔN_{IT} take part in standard charge pumping current at high frequencies. Thus, Equation 6 can be written as:

$$\Delta V_{TH} = \Delta V_{IT} + \Delta V_{OT} \quad (7)$$

Where, ΔV_{OT} is now the voltage shift caused by the oxide-trap increase at high frequency measurements.
After irradiation, I_{CP} (V_B) (where V_B is the base voltage of the gate signal) curves are laterally and vertically shifted. Figure 7 qualitatively illustrates the effect induced by ionizing radiation on CP curves. The lateral shift indicates the introduction of radiation-induced oxide- and interface-trap. However, the vertical one (increase of I_{CPM}) is indicative of the augmentation of interface-trap density, ΔN_{IT} (numbre/cm²).

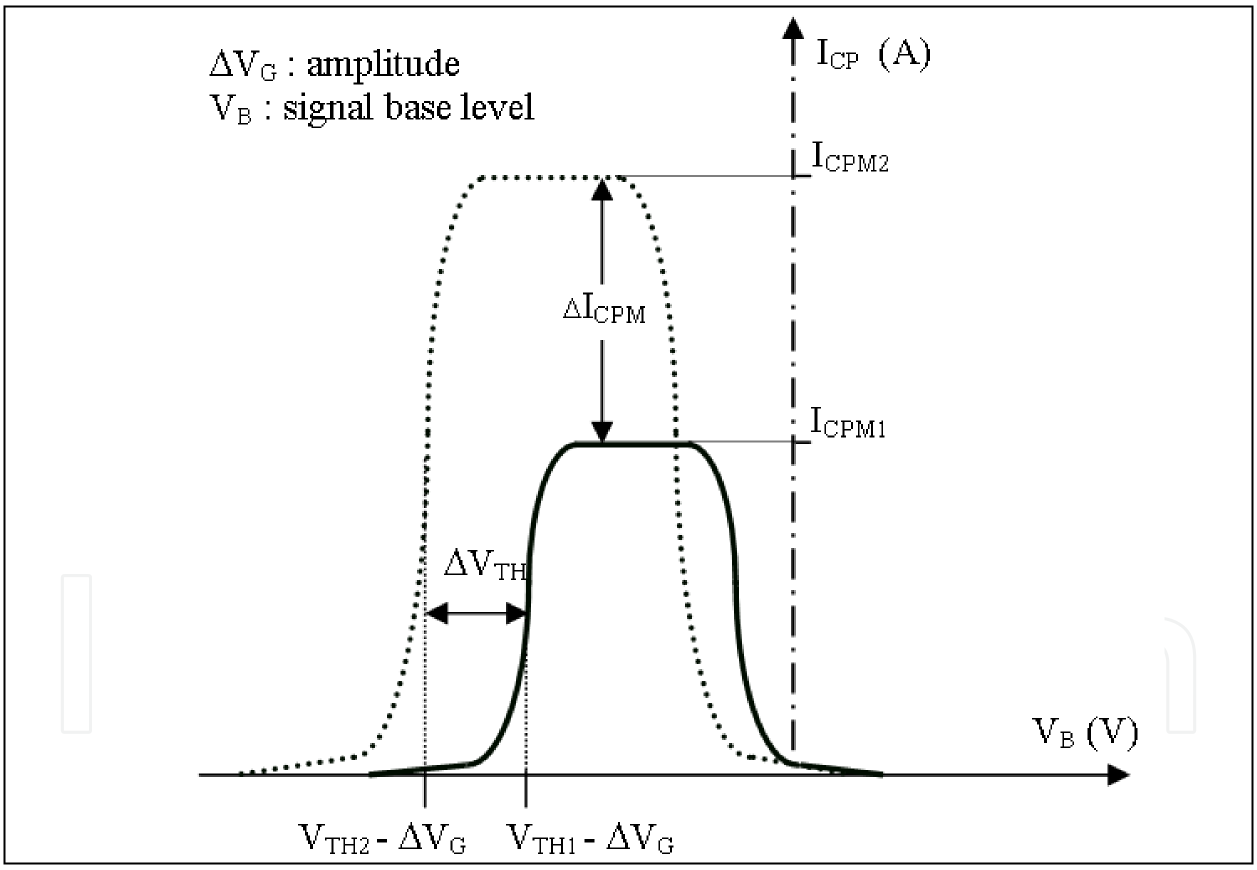

Fig. 7. Schematic illustration of standard charge pumping current curves. Solid line shows CP current before irradiation and Dashed line shows CP current after irradiation.

The I_{CPM} current is given by:

$$I_{CPM} = q.f.A_G.N_{IT} \quad (8)$$

Where,

q (C) is the elementary charge,
N_{IT} (cm^{-2}) is the interface and border-trap densities per area unit,
A_G (cm^2) is the gate area,
f (Hz) is the frequency.

Before irradiation, I_{CPM1} and N_{IT1} represent charge pumping current and interface-trap density respectively. After irradiation, I_{CPM2} and N_{IT2} represent charge pumping current and interface-trap density respectively. Then, the radiation-induced interface-trap density increase (ΔN_{IT}) is given by:

$$\Delta N_{IT} = N_{IT2} - N_{IT1} = \frac{I_{CPM2} - I_{CPM1}}{q.f.A_G} = \frac{\Delta I_{CPM}}{q.f.A_G} \tag{9}$$

Thus, ΔV_{IT} is given by:

$$\Delta V_{IT} = q\frac{\Delta N_{IT}}{C_{OX}} = \frac{\Delta I_{CPM}}{C_{OX}.f.A_G} \tag{10}$$

Using Equations 8 and 12, and $\Delta V_{OT} = -q\ \Delta N_{OT}/C_{OX}$, we have expressed ΔN_{OT}, at high frequencies, as:

$$\Delta N_{OT} = \frac{\Delta I_{CPM}}{q.f.A_G} - \frac{C_{OX}}{q}\Delta V_{TH} \tag{11}$$

where, ΔI_{CPM} (A) is the radiation-induced maximum CP current increase.

5. Experiment

The I_{CP} (V_B) charge pumping measurements were made before and after each irradiation at 25°C. The irradiated NMOS devices were characterized after the latent interface-trap build-up (10^6 s) (Schwank , 1992). In other words, we made a long delay between irradiation and measurements. The I_{CP} (V_B) standard curves (Elliot curves) were extracted using a triangular signal with an amplitude of 3V and a frequency of 100 kHz. The technique consists in varying V_B (signal base voltage) from -6V to 2V. The high frequency value (100 kHz) is chosen basing on Q_{CP} (f) (charge recombined per cycle vs. frequency) measurements performed on our devices. The Q_{CP} (f) characteristics have explicitly shown that the border-traps contribution starts at 10 kHz as frequency as lowered. Consequently, 100 kHz are largely sufficient to avoid their interference with interface-trap.

We expose the experimental results in Fig. 8. All degraded NMOS transistors exhibit the same general features and behaviours as a function of total dose in charge pumping current $I_{CP}(V_B)$ measured by CP technique. When MOSFET transistors are exposed to uniform degradation such as ionizing radiation, the threshold voltage is shifted. This shift is induced by the creation of oxide-trapped charge (ΔQ_{OT}) in the dielectric and interface-trapped charge (ΔQ_{IT}) in the Si/SiO$_2$ system. After irradiation, the curves obtained from CP technique (current measured (I_{CP}) vs. the base voltage of the gate signal (V_B)) are vertically and laterally shifted. The vertical shift represented by the increase of the maximum CP current, I_{CPM}, indicates the augmentation of the interface trap density, ΔN_{IT} (numbre/cm^2) (Fig. 8a).

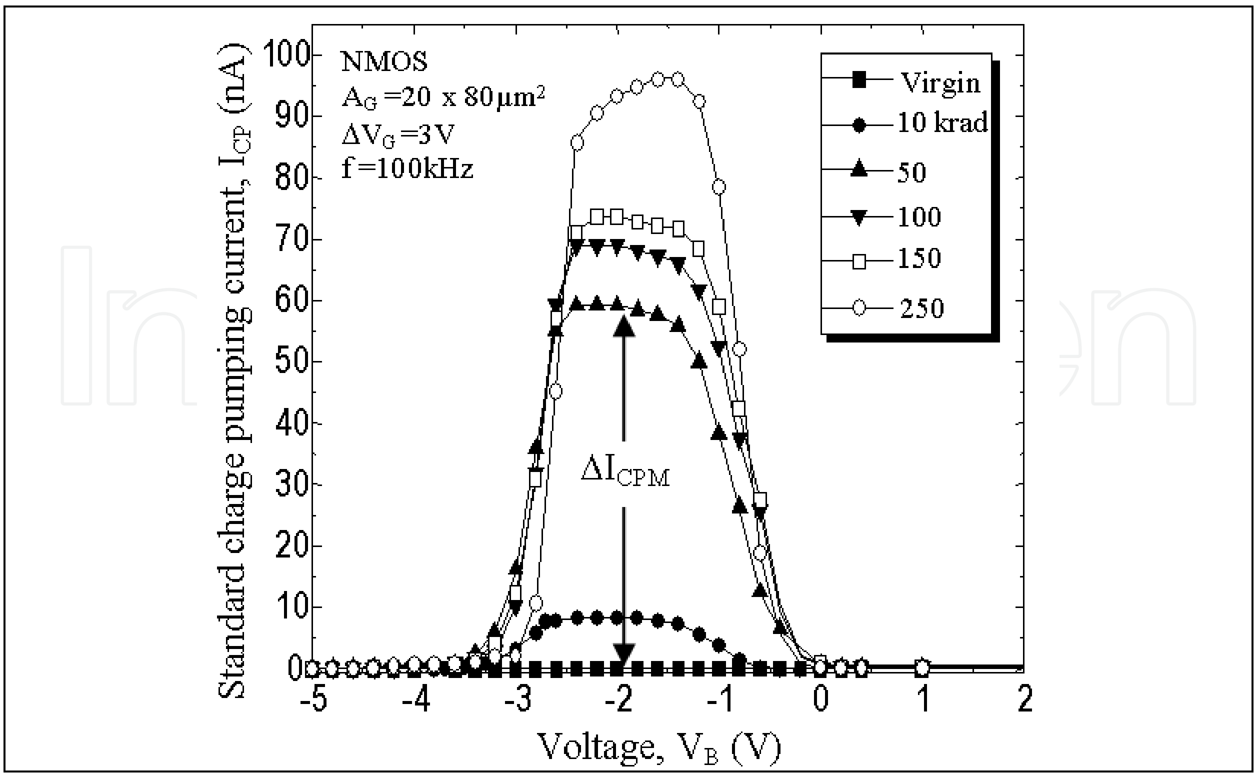

(a)

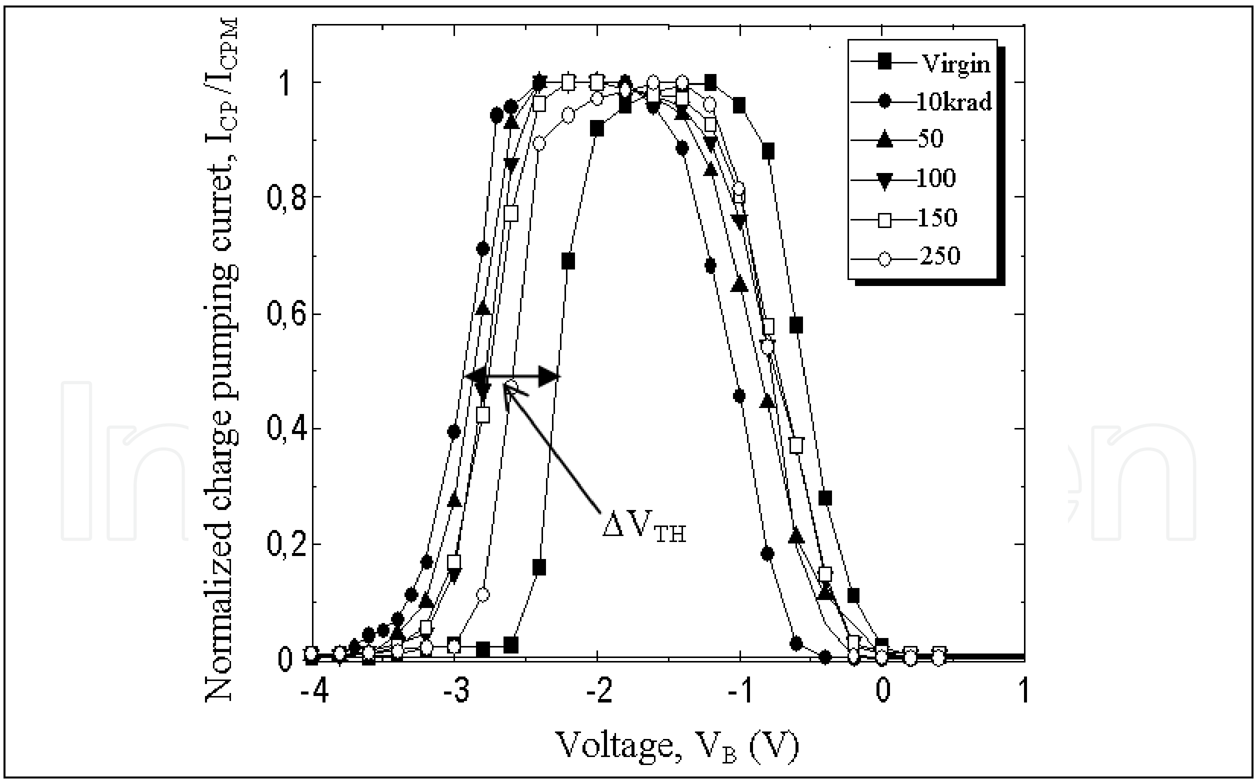

(b)

Fig. 8. Radiation effects on CP curves at high frequencies for different total gamma ray doses. (a) Standard CP current vs. V_B. (b) Normalized CP current vs. V_B.

However, the lateral one indicates the introduction of the radiation-induced oxide- and interface-trap (Fig. 8b). Fig. 8b gives the I_{CP} (V_B) normalized curves to their respective I_{CPM}, in order to illustrate well the lateral shifts induced by irradiation. These quantities are estimated, as shown in figure 8, from I_{CP} (V_B) curves at high frequencies.

Knowing ΔI_{CPM} and ΔV_{TH}, we are able to calculate ΔN_{IT} from equation 9 and also ΔN_{OT} from equation 11. This is very useful when we want to rapidly get information on the quality of irradiated oxide and SiO_2/Si interface and also if we intend to study the annealing of both radiation-induced oxide- and interface-trap.

Equations 9 and 11 shows clearly that ΔN_{IT} and ΔN_{OT} are is just dependent on experimental parameters ΔI_{CPM} and ΔV_{TH} (Djezzar et al., 2004). These quantities are estimated from I_{CP} (V_B) curves at high frequencies.

In Fig. 9, the front panel of the developed software loads two files, of virgin and irradiated MOS devices, respectively and calculates the lateral shift of threshold and flatband voltage, respectively caused by radiation-induced ΔN_{IT} and ΔN_{OT} (normalized charge pumping curves).

The software developed permits to extract the radiation-induced threshold voltage shift (ΔV_{TH}), the radiation-induced flatband voltage shift (ΔV_{FB}), the radiation-induced oxide-trap (ΔN_{OT}), and radiation-induced interface-trap (ΔN_{IT}) are extracted [Oussalah & Djezzar, 2007).

All of the relevant parameters are visible from this screen, as are the experimental results. The program loads a file of a virgin MOS device and extracts the threshold voltage, the flatband and other parameters.

In Fig. 9, we show the window front panel for the charge pumping base level sweep measurement.

The input parameters are:

- file path,
- the signal level,
- the working frequency
- the percentage at the V_{TH} is calculated
- the percentage at V_{FB} is calculated
- process parameters, like, substrate doping (cm^{-3}), oxide capacitor (F/cm^2) and gate oxide area (cm^2).

The extracted parameters by the software are:

- threshold voltage, V_{TH} (V),
- flatband voltage, V_{FB} (V),
- maximum charge pumping current, I_{CPM} (A),
- interface-trapped charge density, Q_{IT} (C/cm^2),
- interface trap density, N_{IT} ($1/cm^2$),
- V_{IT} (V),
- interface trap density, D_{IT} ($1/eV.cm^2$).

In Fig. 10, we show the window front panel for the charge pumping base level sweep measurement for virgin and irradiated MOS transistor. The program loads two files for virgin and irradiated MOS devices, and calculates the lateral shift of V_{TH} and V_{FB}, respectively caused by radiation-induced ΔN_{IT} and ΔN_{OT} (normalized CP curves).

The input parameters in the program software are:

- file path of the virgin MOS transistor,
- file path of the irradiated MOS transistor,
- the signal level,
- the working frequency,

- the percentage at the V_{TH} is calculated,
- the percentage at the V_{FB} is calculated,
- process parameters, like, substrate doping (cm^{-3}), oxide capacitor (F/cm^2) and gate oxide area (cm^2).

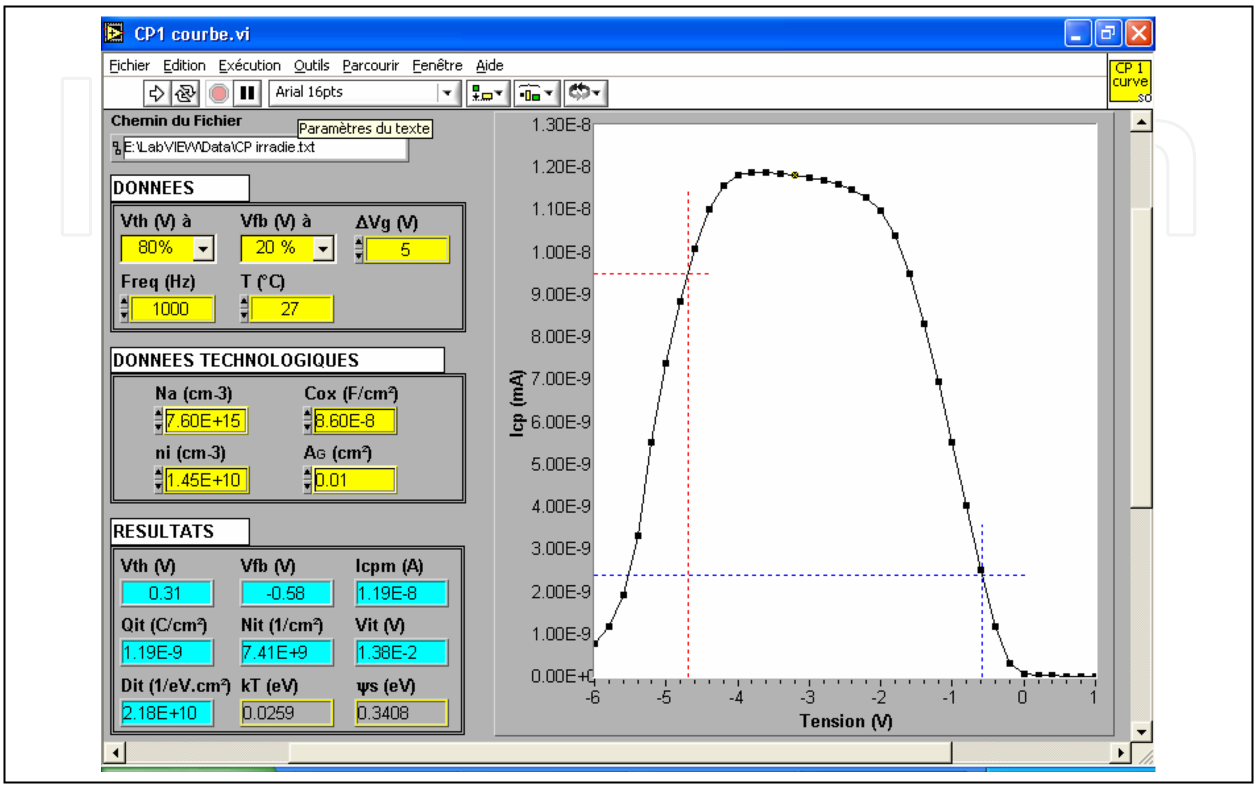
CP1 courbe.vi
Fichier
Edition
Exécution
Outils
Parcourir
Fenêtre
Aide
Arial 16pts
CP 1 curve
Paramètres du texte
1.30E-8
1.20E-8
1.10E-8
1.00E-8
9.00E-9
8.00E-9
7.00E-9
6.00E-9
5.00E-9
4.00E-9
3.00E-9
2.00E-9
1.00E-9
0.00E+0
Icp (mA)
-6
-5
-4
-3
-2
-1
0
1
Tension (V)

Chemin du Fichier
E:\LabVIEW\Data\CP irradie.txt

DONNEES

Vth (V) à 80%
Vfb (V) à 20 %
ΔVg (V) 5
Freq (Hz) 1000
T (°C) 27

DONNEES TECHNOLOGIQUES

Na (cm-3) 7.60E+15
Cox (F/cm²) 8.60E-8
ni (cm-3) 1.45E+10
AG (cm²) 0.01

RESULTATS

Vth (V) 0.31
Vfb (V) -0.58
Icpm (A) 1.19E-8
Qit (C/cm²) 1.19E-9
Nit (1/cm²) 7.41E+9
Vit (V) 1.38E-2
Dit (1/eV.cm²) 2.18E+10
kT (eV) 0.0259
ψs (eV) 0.3408

Fig. 9. LabVIEW front panel for the charge pumping base level sweep measurement.

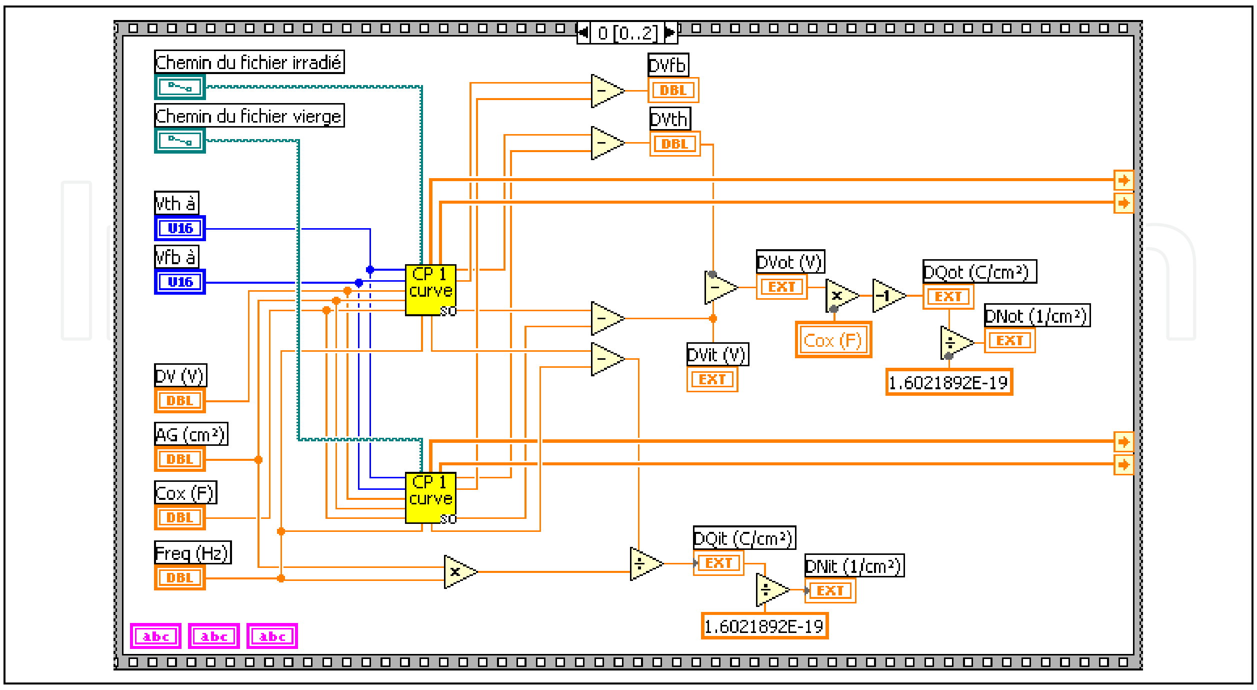
0 [0..2]
Chemin du fichier irradié
Chemin du fichier vierge
Vth à
U16
Vfb à
U16
DV (V)
DBL
AG (cm²)
DBL
Cox (F)
DBL
Freq (Hz)
DBL
abc
abc
abc
DVfb
DBL
DVth
DBL
CP 1 curve
CP 1 curve
DVot (V)
EXT
Cox (F)
DVit (V)
EXT
DQot (C/cm²)
EXT
DNot (1/cm²)
EXT
1.6021892E-19
DQit (C/cm²)
EXT
DNit (1/cm²)
EXT
1.6021892E-19

Fig. 10. LabVIEW diagram panel of figure 9.

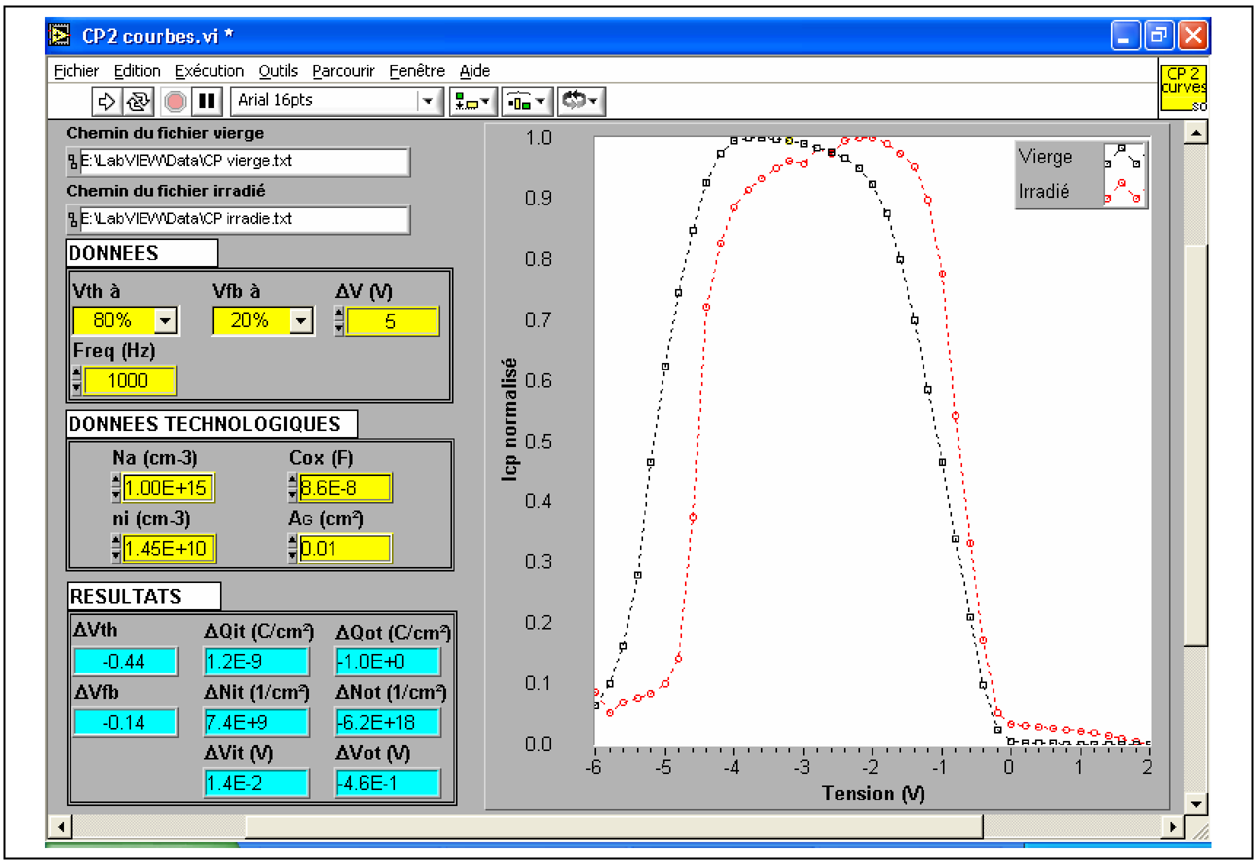

Chemin du fichier vierge
E:\LabVIEW\Data\CP vierge.txt
Chemin du fichier irradié
E:\LabVIEW\Data\CP irradie.txt

DONNEES
Vth à 80%
Vfb à 20%
ΔV (V) 5
Freq (Hz) 1000

DONNEES TECHNOLOGIQUES
Na (cm-3) 1.00E+15
Cox (F) 8.6E-8
ni (cm-3) 1.45E+10
AG (cm²) 0.01

RESULTATS
ΔVth -0.44
ΔQit (C/cm²) 1.2E-9
ΔQot (C/cm²) -1.0E+0
ΔVfb -0.14
ΔNit (1/cm²) 7.4E+9
ΔNot (1/cm²) -6.2E+18
ΔVit (V) 1.4E-2
ΔVot (V) -4.6E-1

Fig. 11. LabVIEW front panel for the radiation induced parameters of the virgin and irradiated MOS transitor.

The extracted parameters by the program software are:

- threshold voltage shift, ΔV_{TH} (V),
- flatband voltage shift, ΔV_{FB} (V),
- oxide trapped charges density, ΔQot (C/cm²),
- Interface trapped charge density, ΔQit (C/cm²).
- Oxide trapped density, ΔNot (1/cm²).
- Interface trapped density, ΔNit (1/cm²).
- Voltage shift caused by interface- trap increase, ΔVit (V).
- Voltage shift caused by oxide-trap increase, ΔV_{OT} (V).

6. Conclusion

Experiments with LabVIEW software have been carried out to determine the effects of gamma radiation at low doses on trap densities in MOSFET devices. The threshold and the flatband voltages degradation due to the charge injection from gamma radiation effect at low doses are characterized with the developed software. Since ΔI_{CPM} and ΔV_{TH} are measured, the program is able to extract ΔN_{IT} and ΔN_{OT}. This is very useful when we want to rapidly get information on the quality of irradiated oxide and SiO_2/Si interface and also if we intend to study the annealing of both radiation-induced oxide- and interface-trap. This makes it a powerful tool for rapid and routinely electrical characterization in hardness assurance test of MOSFET's device qualification for space and strategic applications.

LabVIEW is a powerful environment for software development. It is widely used for instrument control, data acquisition and data analysis. LabVIEW's graphical way of programming allows fast and efficient developing of robust, user controlled applications for measurement, analysis anad visualization of data.

7. References

Doyle, B. S.; Bourcerie, M.; Bergonzoni, C.; Benecchi, R.; Bravis, A.; Mistry, K.R.; & Boudou, A. (1990). The generation and characterization of electron and hole traps created by hole injection during low gate voltage hot-carrier stressing of n-MOS transistors. *IEEE Transactions on Electron Devices*, Vol. 37, (August 1990) 1869-1876.

Tsuchiya, T.; Kobayashi, T.; & Nakajima, S. (1987). Hot carrier-injected oxide region and hot-electron trapping as the main cause in Si nMOSFET degradation. *IEEE Transactions on Electron Devices*, Vol. 34, (February 1987) 386-391.

Chen, I.C.; Holland, S.E. & Hu, C. (1985). Electrical breakdown of thin gate and tunneling oxides. *IEEE Journal of Solid-State Circuits*, Vol. 20, (February 1985) 333-342.

Djezzar, B.; Oussalah, S. & Smatti, A. (2004). A new Oxide-Trap based on Charge Pumping (OTCP) extraction method for irradiated MOSFET devices: part I (high frequencies). *IEEE Transactions on Nuclear Science.* Vol. 51, (August 2004) 1724-1731.

Schwank, J. R.; Fleetwood, D. M.; Shaneyfelt, M. R. & Winokur, P. S. (1993). A critical comparison of charge-pumping, dual-transistor, and midgap measurement techniques. *IEEE Transactions on Nuclear Science.* Vol. 40, (December 1993) 1666-1677.

Groeseneken, G.; Maes, H. E.; Beltran, N. & De Keermaecker, R. F. (1984). A reliable approach to charge pumping measurement in MOS transistors. *IEEE Transactions on Electron Devices*. Vol. 31, (January 1984) 42-53.

Paulsen, R.E.; Siergiej, R.R.; French, M.L. & White, M.H. (1992). Observation of Near-Interface Oxide Traps with the Charge-Pumping Technique. *IEEE Electron Device Letters.*, Vol. 13, N°12, (December 1992) 627-629.

Schroder, D.K. (1998). Semiconductor Material and Device Characterization. John Wiley and Sons, 2nd Edition, New York.

Deal, B.E. (1980). Standardized Terminology for Oxide Charges Associated with Thermally Oxidized Silicon. *Journal of the Electrochemical Society*, Vol. 127, Issue 4, (April 1980) 979-981.

Fleetwood, D. M. (1992). Border Traps in MOS Devices. *IEEE Transactions on Nuclear Science*, Vol. 39, (1992) 269-271.

Oldham, T.R. (1999). *Ionizing Radiation Effects in MOS Oxides*, World Scientific Publishing.

Schwank, J.R.; Fleetwood, D.M.; Shaneyfelt, M.R.; Winokur, P.S.; Axness, C.L. & Riewe, L.C. (1992). Latent Interface-Trap Buildup and its Implications for Hardness Assurance, *IEEE Transactions on Nuclear Science*, Vol. 39, (1992) 1953-1963.

Oussalah, S. & Djezzar, B. (2007). Automated MOS Transistor Degradation Measurements Based on LabVIEW. *Proceedings of the International Conference on design & Technology of Integrated Systems in Nanoscale Era*, Rabat (Morocco), pp. 217-220.

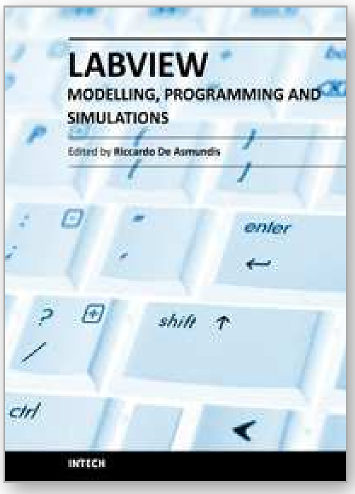
LABVIEW
MODELLING, PROGRAMMING AND SIMULATIONS
Edited by Riccardo De Asmundis
INTECH

Modeling, Programming and Simulations Using LabVIEW™ Software
Edited by Dr Riccardo De Asmundis

ISBN 978-953-307-521-1
Hard cover, 306 pages
Publisher InTech
Published online 21, January, 2011
Published in print edition January, 2011

Born originally as a software for instrumentation control, LabVIEW became quickly a very powerful programming language, having some characteristics which made it unique: simplicity in creating very effective User Interfaces and the G programming mode. While the former allows for the design of very professional control panels and whole applications, complete with features for distributing and installing them, the latter represents an innovative way of programming: the graphical representation of the code. The surprising aspect is that such a way of conceiving algorithms is extremely similar to the SADT method (Structured Analysis and Design Technique) introduced by Douglas T. Ross and SofTech, Inc. (USA) in 1969 from an original idea by MIT, and extensively used by the US Air Force for their projects. LabVIEW enables programming by implementing directly the equivalent of an SADT "actigram". Apart from this academic aspect, LabVIEW can be used in a variety of forms, creating projects that can spread over an enormous field of applications: from control and monitoring software to data treatment and archiving; from modeling to instrument control; from real time programming to advanced analysis tools with very powerful mathematical algorithms ready to use; from full integration with native hardware (by National Instruments) to an easy implementation of drivers for third party hardware. In this book a collection of applications covering a wide range of possibilities is presented. We go from simple or distributed control software to modeling done in LabVIEW; from very specific applications to usage in the educational environment.

How to reference
In order to correctly reference this scholarly work, feel free to copy and paste the following:

Slimane Oussalah and Boualem Djezzar (2011). Automated MOS Transistor Gamma Degradation Measurements Based on LabVIEW Environment, Modeling, Programming and Simulations Using LabVIEW™ Software, Dr Riccardo De Asmundis (Ed.), ISBN: 978-953-307-521-1, InTech, Available from: http://www.intechopen.com/books/modeling-programming-and-simulations-using-labview-software/automated-mos-transistor-gamma-degradation-measurements-based-on-labview-environment

INTECH
open science | open minds

InTech Europe
University Campus STeP Ri
Slavka Krautzeka 83/A
51000 Rijeka, Croatia

InTech China
Unit 405, Office Block, Hotel Equatorial Shanghai
No.65, Yan An Road (West), Shanghai, 200040, China
中国上海市延安西路65号上海国际贵都大饭店办公楼405单元

www.intechopen.com

Phone: +385 (51) 770 447
Fax: +385 (51) 686 166
www.intechopen.com

Phone: +86-21-62489820
Fax: +86-21-62489821

© 2011 The Author(s). Licensee IntechOpen. This chapter is distributed under the terms of the Creative Commons Attribution-NonCommercial-ShareAlike-3.0 License, which permits use, distribution and reproduction for non-commercial purposes, provided the original is properly cited and derivative works building on this content are distributed under the same license.